

Electron transport in two-dimensional arrays

Julia S. Meyer¹, Alex Kamenev¹, and Leonid I. Glazman^{1,2}
¹*Department of Physics, and* ²*W.I. Fine Theoretical Physics Institute,*
University of Minnesota, Minneapolis, MN55455, USA
(Dated: October 29, 2018)

We study charge transport in a granular array with high inter-grain conductances. We show that the system exhibits a Berezinskii-Kosterlitz-Thouless crossover from the high-temperature conducting state into a low-temperature insulating state. The crossover takes place at a critical temperature $T_{\text{BKT}} \propto E_c \exp\{-g\}$, where E_c is the charging energy of a grain and $g \gg 1$ is the dimensionless inter-grain conductance. A uniformly applied gate voltage drives the insulator into a conducting charge liquid state followed by an insulating lattice-pinned Wigner crystal state at larger values of the gate voltage. Technically, we establish correspondence between the charge and phase representations, employing the instanton gas summation in the framework of the phase model.

PACS numbers: 73.23.-b, 73.23.Hk, 71.45.Lr, 71.30.+h

I. INTRODUCTION

Granular arrays have recently attracted much attention as analytically tractable systems to study the interplay of interactions and scattering^{1,2,3,4,5}. The advantage of granular systems is the possibility to separate the scattering-induced quantum interference phenomena from electron-electron interaction effects. Quantum coherence is relevant as long as the typical dwell-time in a grain $\tau_{\text{dwell}} \sim \hbar/(g\delta)$ is longer than the dephasing time τ_φ . Here g is the dimensionless inter-grain conductance measured in units of $e^2/(2\pi\hbar)$, and δ is the mean level spacing of the grains. For two-dimensional disordered interacting systems the dephasing time is known to be⁶ $\tau_\varphi \approx \hbar g/T$. The quantum interference is thus suppressed if $\tau_\varphi < \tau_{\text{dwell}}$, which is the case at $T > g^2\delta$. Hereafter we assume this condition to be satisfied and consider the temperature range $g^2\delta < T < E_c$ (where $E_c = e^2/(2C)$ is the charging energy of the grains). This allows us to focus on the interaction-induced phenomena, while omitting the interference (incoherent regime).

Earlier studies of incoherent two-dimensional arrays led to conflicting theoretical results^{4,7,8}. In Refs. [7,8] the low-temperature insulating state was found for sufficiently small inter-grain conductance, $g < 1$. Upon elevating the temperature, the array was shown to undergo a Berezinskii-Kosterlitz-Thouless (BKT) transition into the conducting state. The transition temperature $T_{\text{BKT}} = T_{\text{BKT}}(g)$ was predicted to go to zero at some critical value of conductance $g_c \approx 1.8$. At larger conductances, $g > g_c$, the metallic state was claimed to persist down to zero temperature. In Ref. [4] the same model as in Refs. [7,8] was studied in the regime of large conductances, $g \gg 1$. Using a perturbative renormalization group (RG) analysis, the renormalized inter-grain conductance was shown to behave as $g \Rightarrow g(T) = g - \frac{2}{d} \ln(E_c g/T)$ (where $2d$ is the coordination number of the lattice). This correction is essentially similar (and at $T \approx g\delta$ crosses over⁹) to the interaction-induced Altshuler-Aronov¹⁰ conductivity corrections known for homogeneous disordered sys-

tems. At $T \sim E_c g \exp\{-dg/2\}$, the conductance is renormalized down to $g(T) \sim \mathcal{O}(1)$. Thus, one may expect that the system approaches an insulating state at low enough temperature even for large bare inter-grain conductance. Whether such a “high- g ” insulator indeed exists, and – if so – its nature and relation (if any) to the BKT transition, found^{7,8} for “low- g ” systems, was not clarified.

In the present work we show how to reconcile these findings. In particular, we show that there exists a finite $T_{\text{BKT}} \propto \exp\{-g\}$ at $g \gg 1$. To this end one needs to go beyond the perturbative analysis⁴ of the model considered in Refs. [4,7,8] and include non-perturbative – instanton – field configurations. A similar program was recently carried out for one-dimensional incoherent arrays⁵. The conductivity of one-dimensional arrays was found to display activated (insulating) behavior with the charge gap $\sim E_c \exp\{-g/4\}$, which is parametrically larger than the temperature where the perturbative corrections become large. It was also shown that the proper low-temperature representation of incoherent arrays is that of pinned charge-density wave fluctuations. [This should be contrasted with the fluctuating phase (or voltage) picture employed in Refs. [4,7,8].] The activation gap corresponds to the energy needed to create a long unit-charge soliton.

In the present paper the charge representation is derived and analyzed for the two-dimensional setup. We find that the charge excitations are localized unit-charge two-dimensional solitons. At $g \gg 1$ the solitons interact logarithmically over a large range of distances. This leads to a sharp BKT crossover^{11,12} between a low-temperature insulating phase with bound charge-anti-charge pairs (and an exponentially small number of free charges) and a high-temperature conducting phase, where the pairs are unbound. The BKT temperature $T_{\text{BKT}}(g)$ remains finite (though exponentially small), $T_{\text{BKT}}(g) \sim E_c g \exp\{-g\}$, for an *arbitrarily high* bare conductance g . The zero-temperature quantum phase transition at $g = g_c$, found in Refs. [7,8], thus, does *not* exist. Instead, there is a fast but continuous drop of the

transition temperature $T_{\text{BKT}}(g)$ in the vicinity of $g \sim 1$.

The issue of whether a classical phase transition or a crossover occurs as the temperature is lowered, depends sensitively on the details of the model. The true BKT transition takes place only if the interactions between the charged solitons are logarithmic at arbitrarily large distances. This is the case for arrays with inter-grain capacitances only (in the absence of the grain's self-capacitance, no electric field lines can leave the 2d plane). In the presence of the self-capacitance, the interaction is logarithmic in a wide, but finite range of distances: $1 < l \lesssim \exp\{g/2\}$ (hereafter distances are measured in units of the array lattice spacing). In the latter case, below the BKT temperature the array's conductivity is not zero (in contrast to the former case), but rather exhibits the activation behavior,

$$\sigma \simeq g \exp\left\{-\frac{\Delta}{T}\right\}, \quad (1)$$

where the activation gap is given by $\Delta \simeq gT_{\text{BKT}} \gg T_{\text{BKT}}$. Upon raising the temperature, above the BKT temperature the conductivity sharply increases as

$$\sigma = gK \exp\left\{-2b\sqrt{\frac{T_{\text{BKT}}}{T - T_{\text{BKT}}}}\right\}, \quad (2)$$

where K and b are non-universal constants of order unity¹³. Finally, above the transition region, the conductivity crosses over to the perturbative prediction $\sigma = g - \ln(gE_c/T)$. We thus have a generally consistent picture based on the BKT physics at any value of bare conductance, g .

A gate voltage induces a uniform background charge $q \in [0, 1]$. However, for small gate voltages the array remains in the particle-hole symmetric state with an integer number of electrons per dot. The transition into a non-uniform state (with a non-integer average number of electrons per dot) takes place at a critical dimensionless charge density $q^* = \Delta/(2E_c)$. Its physics is similar to the transition from the Meissner to the Abrikosov state in type II superconductors upon increasing an external magnetic field. In our case the role of the magnetic field is played by the gate voltage, q , with q^* corresponding to the lower critical field H_{c1} . The Abrikosov lattice in turn corresponds to the 2d Wigner crystal formed by the unit-charge solitons. Such a crystal is easily pinned by the lattice. Consequently, at low temperatures, the array is in the insulating phase with a residual activation conductivity, associated with the thermal creation of defects. The Wigner crystal melts at a temperature¹⁴ of the order of T_{BKT} , leading to a sharp crossover into the conducting phase.

Methodologically, interacting systems may be modeled in two alternative ways: in terms of either phase or charge degrees of freedom. The two are canonically conjugated and the choice between them is a matter of convenience. The phase representation is easier to derive microscopically starting from the fermionic tunneling Hamiltonian.

By this reason it was used in the vast majority of works on granular systems and quantum dots^{2,3,4,7,8}. We found it more convenient, however, to work in the charge representation, which is the natural language to describe the insulating phase. In the quantum dot context, the charge description was introduced in Refs. [15,16]. Here we employ its generalization to 2d granular arrays. We introduce the model in Sec. II and show that it exhibits the BKT crossover in Sec. III. Finite gate voltages and the pinned Wigner crystal phase are discussed in Sec. IV. To facilitate comparison with the body of work on the phase representation, we include the proof of equivalence of the two models in Appendix B.

II. CHARGE REPRESENTATION

In this section, we introduce the charge representation for incoherent ($\delta \rightarrow 0$) interacting arrays. To keep the presentation compact, we assume all contacts to be single-channel, characterized by a reflection amplitude $r < 1$. The generalization to the multichannel case and, in particular, to $g \gg 1$ is discussed at the end of the section and, in more detail, in Appendix A, while the proof of the equivalence of the resulting charge model to the more widely used phase model is outlined in Appendix B.

A. Single contact

Consider a point contact between a quantum dot and a metallic reservoir. Such a point contact allows for a small number of propagating transverse modes which may be thought of as one-dimensional electron liquids (with the contact situated at the origin, $z = 0$). Here we consider the case of a single propagating mode, deferring the consideration of multi-mode contacts to Appendix A. The corresponding one-dimensional electron liquid may be bosonized in the conventional way^{15,16} and described in terms of the bosonic field $\theta(\tau, z)$. Its gradient $\partial_z\theta(\tau, z)$ has the meaning of a local electron density. As a result, the electron number on the dot may be written as $N = \int_0^\infty dz \partial_z\theta(\tau, z) = -\theta(\tau, 0)$ and, thus, the Coulomb energy takes the form $(eN)^2/(2C) = E_c\theta^2(\tau, 0)$. Finally the imaginary-time action of the bosonic field reads

$$S[\theta(\tau, z)] = \int_0^\beta d\tau \left\{ \int_{-\infty}^\infty dz [(\partial_\tau\theta)^2 + (\partial_z\theta)^2] + E_c\theta^2(\tau, 0) - \frac{Dr}{\pi} \cos[2\pi\theta(\tau, 0)] \right\}. \quad (3)$$

The last term in this expression describes backscattering at the point contact with the reflection amplitude r , while D is the electronic bandwidth.

One may integrate out all degrees of freedom with $z \neq 0$, retaining the field $\theta(\tau) \equiv \theta(\tau, 0)$ only. The corre-

sponding action reduces to

$$S[\theta] = \frac{1}{T} \sum_m \left(\pi |\omega_m| \theta_m^2 + E_c \theta_m^2 \right) - \frac{Dr}{\pi} \int_0^\beta d\tau \cos(2\pi\theta(\tau)), \quad (4)$$

where $\omega_m = 2\pi Tm$, and we have introduced the Matsubara representation though the transformation $\theta_m = \int_0^\beta d\tau \theta(\tau) e^{-i\omega_m \tau}$. The dissipative term, $\pi |\omega_m| \theta_m^2$, is generated as a result of integrating out the continuum spectrum of the degrees of freedom on the dot. Its appearance is a consequence of the assumption that the mean level spacing is the smallest energy scale in the model, $\delta \rightarrow 0$.

B. 2d array

We now generalize the single-contact action, Eq. (4), to the 2d array geometry. To this end we introduce the vector index \mathbf{l} to label the grains. We also introduce two fields $\theta_{x,\mathbf{l}}(\tau)$ and $\theta_{y,\mathbf{l}}(\tau)$ which describe charge transport from grain \mathbf{l} in the positive x and y directions, respectively. In these notations, the instantaneous electron density on the grain \mathbf{l} is given by the lattice divergence $\nabla \cdot \vec{\theta}_{\mathbf{l}} \equiv \theta_{x,\mathbf{l}+\mathbf{e}_x} - \theta_{x,\mathbf{l}} + \theta_{y,\mathbf{l}+\mathbf{e}_y} - \theta_{y,\mathbf{l}}$ (cf. Fig. 1). With the backscattering in the contact, characterized by the reflection amplitude r , the action reads

$$S[\vec{\theta}] = \sum_{\mathbf{l}} \left\{ \frac{1}{T} \sum_m \left(\pi |\omega_m| \vec{\theta}_{\mathbf{l},m}^2 + E_c (\nabla \cdot \vec{\theta}_{\mathbf{l},m})^2 \right) - \frac{Dr}{\pi} \sum_{i=x,y} \int_0^\beta d\tau \cos(2\pi\theta_{i,\mathbf{l}}(\tau)) \right\}, \quad (5)$$

where D is again the bandwidth. As in Eq. (4), the first term in the action (5) describes the dissipative dynamics originating from integrating out degrees of freedom within the grains, the second term is responsible for the charging, and the third one describes backscattering in the contacts.

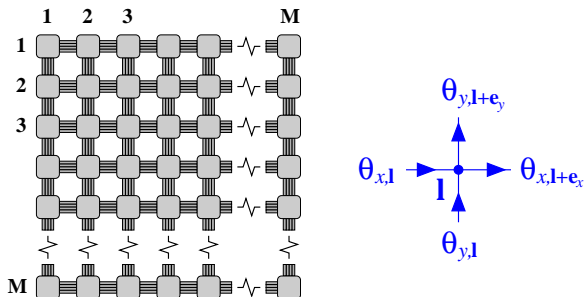


FIG. 1: Granular array with a square lattice. The massless modes η , explained in the text, correspond to circular currents around a plaquette and, therefore, do not contribute to charge transport.

For a square lattice of linear size M , the array contains M^2 grains and $2M^2$ contacts between them. Consequently the model is written in terms of $2M^2$ bosonic degrees of freedom, $\theta_{i,\mathbf{l}}(\tau)$. In the limit $r \rightarrow 0$, the masses of these modes are provided only by the M^2 charging terms $E_c (\nabla \cdot \vec{\theta}_{\mathbf{l},m})^2$. Therefore, if the backscattering is neglected, only half of the degrees of freedom of the model are massive. To see this explicitly, one may rewrite the 2d vector field $\vec{\theta}$ through two scalar fields $\vec{\theta} = \nabla\chi + \nabla \times \eta$ and notice that the charging term contains only the field χ while the curl-field η fully decouples from it.

In order to find an effective low-energy theory, we shall proceed with the renormalization group (RG) scheme

based on the integration of the high frequency Matsubara modes, $D' < |\omega_m| < D$, accompanied by the appropriate change of the backscattering amplitude r . As long as the coefficient in front of the cosine-term in Eq. (5) is less than the running bandwidth D' , one may treat the fields as Gaussian, governed by the first two terms in Eq. (5). As a result, the backscattering amplitude renormalizes as

$$Dr \Rightarrow Dr \exp \left\{ -\frac{(2\pi)^2}{2} \langle \theta_i^2 \rangle \right\}, \quad (6)$$

where the averaging in $\langle \theta_i^2 \rangle$ is performed over high-frequency fluctuations. Passing to the momentum representation and taking into account both χ and η components of the fluctuations, one finds

$$\begin{aligned} \langle \theta_i^2 \rangle &= \frac{T}{4M^2} \sum_{|\omega_m|=D'}^D \sum_{q_x, q_y=1}^M \left(\frac{1}{E_{\mathbf{q}} + \pi |\omega_m|} + \frac{1}{\pi |\omega_m|} \right) \\ &\simeq \frac{1}{4\pi^2} \left(\ln \frac{D}{E_c} + \ln \frac{D}{D'} \right) = \frac{1}{2\pi^2} \ln \frac{D}{\sqrt{E_c D'}}, \end{aligned} \quad (7)$$

where $E_{\mathbf{q}} = 4E_c \sum_{i=x,y} \sin^2(\pi q_i / (2M))$ is the mass spectrum of the χ modes. In the second line we have assumed that $D' < E_c$ (in the opposite case, $D' > E_c$, one should substitute $\sqrt{E_c D'}$ by D'). Notice that the presence of the lower limit, D' , in this expression is due to the massless rotational modes of the field η . [Note also the difference with the 1d-system, where all modes are massive and, therefore, the result corresponding to Eq. (7) is independent on the lower limit⁵.] Combining Eqs. (6) and (7), one finds that upon integrating out the high-frequency modes, the coefficient of the cosine potential renormalizes as $Dr \Rightarrow \sqrt{E_c D'} r$. As was discussed above, this procedure works as long as $\sqrt{E_c D'} r < D'$, that is

$D' > T_0$, where $T_0 = E_c r^2$ is the “freezing” temperature. For smaller bandwidths, the cosine-term itself provides a mass for the rotational modes η . As a result, all modes acquire a mass and, thus, the renormalized backscattering amplitude loses its sensitivity to the lower limit D' . Therefore, we arrive at the conclusion that for $D' < T_0$ the cosine amplitude saturates at a value about T_0 . Integrating in this way all Matsubara components, except the static one, $m = 0$ (it is obvious from Eq. (7) that the $m = 0$ component can not be handled in the same way), one obtains an effective classical model with the action

$$S_{\text{cl}}[\vec{\theta}] = \frac{E_c}{T} \sum_{\mathbf{l}} \left\{ (\nabla \cdot \vec{\theta}_{\mathbf{l}})^2 - \frac{\gamma(T)}{2\pi^2} \sum_{i=x,y} \cos(2\pi\theta_{i,\mathbf{l}}) \right\}, \quad (8)$$

where $\gamma(T) = 2\pi\sqrt{T/E_c} r$ for $T > T_0$ and $\gamma(T) \simeq 2\pi r^2$ for $T < T_0$.

So far we have formulated the model for an array with single-channel contacts. Generalization to the $N \geq 2$ channels is achieved by introducing bosonic modes $\vec{\theta}_{1,\alpha}(\tau)$ for every channel $\alpha = 1 \dots N$. One may then integrate out the antisymmetric modes (including the spin modes) for every contact, retaining only the symmetric (charge) mode $\vec{\theta}_{\mathbf{l}} = \sum_{\alpha=1}^N \vec{\theta}_{1,\alpha}$, see Appendix A for details. The main result of such a procedure may be summarized by the redefinition of the effective backscattering amplitude^{17,18} $r \Rightarrow c_N \prod_{\alpha=1}^N r_{\alpha}$ in the action of the charge mode (c_N is a numerical coefficient with a finite limit c_{∞}). Consequently the characteristic freezing temperature changes to $T_0 \simeq E_c \prod_{\alpha=1}^N r_{\alpha}^2$. Then, the charge mode may be described by the same effective classical model Eq. (8) with $\gamma(T) \simeq \sqrt{T/E_c} \prod_{\alpha=1}^N r_{\alpha}$ for $T > T_0$ and $\gamma(T) \simeq \prod_{\alpha=1}^N r_{\alpha}^2$ for $T < T_0$.

A model which adequately describes an array of metallic grains assumes that the contacts between grains consist of a large number N of weakly transmitting channels^{2,3,4,7,8}. For sufficiently large N , the total conductances of the junctions may still be high, $g = \sum_{\alpha=1}^N t_{\alpha}^2 > 1$, where $t_{\alpha}^2 = 1 - r_{\alpha}^2 \ll 1$ is the transmission probability in channel α . In this case, one finds that $\prod_{\alpha} r_{\alpha} = \exp\{\frac{1}{2} \sum_{\alpha} \ln(1 - t_{\alpha}^2)\} \approx \exp\{-g/2\}$. Employing the expressions derived above, one obtains that the freezing temperature is of the order $T_0 \simeq g E_c e^{-g}$, while the effective amplitude of the cosine potential in Eq. (8) is given by

$$\gamma(T) \simeq \begin{cases} \sqrt{g} e^{-g/2} \sqrt{\frac{T}{E_c}}; & T > T_0, \\ g e^{-g}; & T < T_0. \end{cases} \quad (9)$$

In Appendix B, we show how Eqs. (8) and (9) follow from the phase model^{2,3,4,7,8}, demonstrating that the two models based on the charge and phase representations, respectively, are reduced to the same effective classical system. Notice that, since the charge model was derived for $r_{\alpha} \ll 1$, while $t_{\alpha} \ll 1$ is assumed in the phase model, the coincidence of $\gamma(T)$ may be expected at best with exponential accuracy. The algebraic pre-exponential func-

tion of g is a result of the evaluation in the framework of the phase model, see Appendix B.

III. BKT TRANSITION

In this Section we analyze the physics of the classical charge model specified by Eqs. (8) and (9). Two issues are discussed: (i) the spectrum of its charged excitations and their interactions, and (ii) the low-frequency charge dynamics and the dc conductivity of the array. We finally put our findings in perspective by comparing them with the results of previous studies.

A. Charge spectrum

The lowest energy configuration of the action (8) is given by $\vec{\theta} = 0 \pmod{1}$ everywhere. Localized excitations must have integer $\vec{\theta}$ far away from the core to minimize the cosine potential. The total charge of such localized excitation is $e \int (d^2l) \nabla \cdot \vec{\theta} = e \int d\vec{s} \cdot \vec{\theta}$, where the line integral on the r.h.s. is calculated over a distant contour enclosing the excitation. It is clear therefore that the charge of the excitation is quantized in integer numbers of e . The simplest (and only stable) charged excitations have charge $\pm e$. They consist of a large (i.e., spread out over $\sim 1/\gamma \gg 1$ grains) localized 2d soliton of unit charge, connected to a 1d string of links with $\theta_i = 1$. The other end of the string may either go to the system boundary or be terminated by an anti-soliton with charge $-e$. The soliton solution centered at $\mathbf{l} = 0$ can be written in the form $\vec{\theta}_{\mathbf{l}} = 1 - \vec{\vartheta}(\mathbf{l})$ for the links along the string and $\vec{\theta}_{\mathbf{l}} = \vec{\vartheta}(\mathbf{l})$ everywhere else, where $|\vec{\vartheta}(|\mathbf{l}| \rightarrow \infty)| \rightarrow 0$. Minimizing the action, Eq. (8), with respect to $\vec{\vartheta}$, one finds the saddle point equation for the soliton solution,

$$\nabla(\nabla \cdot \vec{\vartheta}) - \frac{\gamma}{2\pi} \sum_{i=x,y} \sin(2\pi\vartheta_i) \mathbf{e}_i = 0. \quad (10)$$

Except for a domain consisting of $\mathcal{O}(1)$ links closest to the core of the soliton, ϑ is small, justifying an expansion of the sine-term in the saddle point equation. As a result, Eq. (10) takes the form $\nabla(\nabla \cdot \vec{\vartheta}) - \gamma \vec{\vartheta} = 0$. Its unit-charge solution is:

$$\vec{\vartheta}(\mathbf{l}) = -\frac{\sqrt{\gamma}}{2\pi} K_1\left(\frac{l}{\xi_s}\right) \mathbf{e}_l, \quad (11)$$

where K_1 is a modified Bessel function, and $\xi_s = 1/\sqrt{\gamma} \gg 1$, justifying the continuum approximation; finally $\mathbf{e}_l \equiv \mathbf{l}/l$. The solution is normalized as $\int (d^2l) \nabla \cdot \vec{\theta} = 1$ to obey the charge quantization.

Substituting this solution back into the action, Eq. (8), one finds that the soliton energy originates primarily from the cosine potential part of the action and is given by $\Delta \simeq E_c [\gamma(T)/2\pi] \ln \xi_s$. The large logarithmic factor $\ln \xi_s = -\frac{1}{2} \ln \gamma \gg 1$ is due to the $\propto 1/l^2$ behavior of the

charge density in the wide range of distances $1 < l < \xi_s$. At larger distances, $l > \xi_s$, the charge density decays exponentially. As a result, the solitons interact logarithmically up to a distance ξ_s beyond which the interaction is exponentially screened. Since the density of thermally-excited solitons is $n_s \approx \exp\{-\Delta/T\}$, the mean distance between them is $l_s = n_s^{-1/2} \approx \exp\{\Delta/(2T)\}$. It becomes comparable to ξ_s at $T \approx \Delta/(2 \ln \xi_s) = E_c \gamma(T)/(4\pi)$. This condition is satisfied at temperatures about the “freezing” temperature, $T \sim T_0$. Thus, at $T < T_0$, the thermally-excited charges are essentially non-interacting, while, at $T > T_0$, there is a neutral (in average) gas of logarithmically interacting solitons and anti-solitons.

In the latter regime the partition function of the charged degrees of freedom may be written therefore as

$$Z = \sum_{n=0}^{\infty} \frac{f^n}{n!} \int (d^2 l_1) \dots (d^2 l_n) e^{\pm \frac{E_c \gamma(T)}{2\pi T} \sum_{k,k'}^n \ln |l_k - l_{k'}|}, \quad (12)$$

where $\ln f \simeq E_c \gamma(T)/T$ is the fugacity of the logarithmic gas, originating from the solitons core energy. The plus/minus signs in the exponent correspond to soliton-soliton and soliton-anti-soliton interactions, respectively.

It is well known that the Coulomb gas in 2d described by Eq. (12) undergoes the BKT transition^{11,12} at a critical temperature $T_{\text{BKT}} \approx E_c \gamma/(4\pi)$. For $T < T_{\text{BKT}}$, the charges are bound in charge-anti-charge pairs. The residual density of free charges is exponentially small and given by $n_s \approx \exp\{-\Delta/T\}$, where $\Delta = T_{\text{BKT}} \ln \xi_s^2$. The value of Δ is finite but large, as long as the solitons interact with each other logarithmically over a broad range of distances $\xi_s \gg 1$. Notice that the Coulomb interactions in our model are strictly on-site (only the self-capacitance, C , is included). The long range of the soliton-soliton interactions is due to the fact that in a strongly coupled array, $g \gg 1$, the charge is spread over a large distance $\xi_s \sim \exp\{g/2\}$.

One can modify the model to include mutual capacitances C' between neighboring grains (and thus to include long-range Coulomb interactions). It is straightforward to show that such modification alters the range of logarithmic interactions as $\xi_s \rightarrow \xi_s \sqrt{1 + C'/C}$, while the charging energy now reads $E_c = e^2/(2(C + C'))$. In the limit $C \rightarrow 0$, while C' remains finite, the interaction range diverges, $\xi_s \rightarrow \infty$. In fact, this was to be anticipated: since without the self-capacitance no electric field lines can leave the system, one deals with the true 2d Coulomb interaction, which is logarithmic. In this case $\Delta \rightarrow \infty$ and the density of free charges below T_{BKT} is strictly zero. This is the case of the genuine BKT phase transition. For non-vanishing self-capacitance, $C > 0$, the interactions are screened at distances exceeding ξ_s . Therefore, the density of free charges is finite at any temperature and the phase transition is smeared into a sharp crossover. Above the transition/crossover temperature the density of free charges rapidly increases as¹¹ $n_s \sim \exp\{-2b\sqrt{T_{\text{BKT}}/(T - T_{\text{BKT}})}\}$, where b is a constant of order unity, driving the array into the conducting

phase.

B. dc conductivity

In order to discuss the dc conductivity of the array, one needs to restore the low frequency, $\omega \ll T$, dynamics of the classical charge model, Eq. (8). This may be done formally by keeping the dissipative dynamical term in the action. Notice that in the multichannel case, see Appendix A, the coefficient in front of $|\omega_m|$ acquires a factor N^{-1} , where N is the number of channels. In the presence of strong backscattering, it actually reads $\pi g^{-1} |\omega_m| \vec{\theta}_{1,m}^2$ and corresponds to the conventional Ohmic dissipation. Since we focus on the low frequencies, it is convenient to pass to the Keldysh representation (to avoid dealing with the analytical continuation) and consider its semi-classical limit. The latter is known to be equivalent to a certain Langevin dynamics¹⁹.

Here we prefer to take a more phenomenological route, leading to the same conclusions. Let us consider the static equations of motion following from Eq. (8): $\partial_i \left(\frac{e}{C} \nabla \cdot \vec{\theta}_1 \right) - \frac{e\gamma}{2\pi C} \sin(2\pi\theta_{i,1}) = 0$. Since $\frac{e}{C} \nabla \cdot \vec{\theta}_1 \equiv V_1$ is the voltage on grain \mathbf{l} , the equation simply expresses the fact that in the absence of charge quantization, $\gamma \rightarrow 0$, all grains are equipotential: $\nabla V_1 = V_{1+\mathbf{e}_i} - V_1 = 0$. Once currents are allowed to flow in the array this condition should be substituted by the Kirchhoff law, $V_{1+\mathbf{e}_i} - V_1 = RI_{i,1}$, where $R = 2\pi\hbar/(e^2g)$ is the contact resistance, and $I_{i,1} = e\partial_t\theta_{i,1}$ is the current flowing between grains \mathbf{l} and $\mathbf{l} + \mathbf{e}_i$. Restoring also the γ -term in the equation of motion, one thus finds

$$\begin{aligned} & \frac{\pi}{g} \partial_t \vec{\theta} - E_c \left[\nabla(\nabla \cdot \vec{\theta}) - \frac{\gamma}{2\pi} \sum_i \mathbf{e}_i \sin(2\pi\theta_i) \right] \\ &= -\frac{e}{2} \mathbf{E} + \vec{\xi}(t). \end{aligned} \quad (13)$$

On the right hand side we have included an external electric field \mathbf{E} , as well as the Gaussian noise, $\vec{\xi}(t)$, with the correlator

$$\langle \xi_{i,1}(t) \xi_{i',1'}(t') \rangle = \frac{2\pi T}{g} \delta(t - t') \delta_{1,1'} \delta_{i,i'}, \quad (14)$$

to satisfy the fluctuation-dissipation theorem.

Our goal is to calculate the current, I , in presence of a weak uniform field, E . To this end we employ Drude-type arguments, saying that $I = en_s v$, where n_s is the carrier concentration and v is their drift velocity. The only mobile carriers in the system are the solitons, Eq. (11), whose concentration, n_s , we have discussed in detail above. Now we concentrate on the drift velocity, v . We look for a solution of Eq. (13) (without the noise) in the form $\vec{\theta}(\mathbf{l}, t) = \vec{\theta}_0(\mathbf{l} - \mathbf{v}t) + \vec{\theta}_1(\mathbf{l} - \mathbf{v}t) + \vec{\alpha}$. Here $\vec{\theta}_0(\mathbf{l})$ is the static soliton solution in the absence of the external field, whereas $\vec{\theta}_1 \sim \mathbf{E}$ is a small modification of the soliton's shape due to the presence of the external field. Finally the constant vector $\vec{\alpha}$ is determined

by the shift of the minimum of the periodic potential in the field: $E_c \gamma \sum_i \mathbf{e}_i \sin(2\pi\alpha_i) = \pi \mathbf{E}$. Choosing $\mathbf{E} = E \mathbf{e}_x$ and $\mathbf{v} = v \mathbf{e}_x$, and linearizing Eq. (13), one finds that $\vec{\theta}_1$ satisfies the equation

$$E_c \hat{\mathcal{F}}_{\{\vec{\theta}_0\}} \vec{\theta}_1 = \frac{v}{g} \partial_x \vec{\theta}_0 - \frac{E}{\pi} \sin^2(\pi\theta_{0,x}) \mathbf{e}_x, \quad (15)$$

where $\hat{\mathcal{F}}_{\{\vec{\theta}_0\}} \vec{\theta}_1 \equiv \nabla(\nabla \cdot \vec{\theta}_1) - \gamma \sum_i \mathbf{e}_i \cos(2\pi\theta_{0,i}) \theta_{1,i}$. The velocity, v , is determined by the condition that the r.h.s. of Eq. (15) is orthogonal to the translational zero-mode of the operator $\hat{\mathcal{F}}_{\{\vec{\theta}_0\}}$, given by $\partial_x \vec{\theta}_0$. This requirement leads to $v \sim gE$. Finally, the dc conductivity is given by $\sigma \simeq g n_s(T)$.

As a result, all the conclusions, drawn above, regarding the BKT transition/crossover in the soliton density may be directly translated to the array's conductivity. In particular, for the self-capacitance model at $T < T_{\text{BKT}}$ (employing that at low temperature $\ln \gamma \simeq g$) we find Eq. (1), i.e. $\sigma \simeq g \exp\{-\Delta/T\}$. Above T_{BKT} , the conductivity behaves as $\sigma \simeq g \exp\{-2b\sqrt{T_{\text{BKT}}/(T - T_{\text{BKT}})}\}$, see Eq. (2). At even higher temperatures, this behavior crosses over to the result⁴ of the perturbative calculation, $\sigma = g - \ln(gE_c/T)$.

C. Phase diagram

Using the results of the previous sections, we are now in a position to discuss the phase diagram of the array. An array having inter-grain capacitances C' only exhibits a BKT phase transition between the low-temperature insulating and the high-temperature conducting phases. Its phase diagram on the plane temperature vs. bare inter-grain conductance, g , is shown in Fig. 2. Unlike previous works^{7,8} that predicted a zero-temperature metal for $g > g_c \simeq 1$, we find that the low-temperature phase is an insulator for arbitrarily large g . The critical temperature, $T_{\text{BKT}}(g)$, however, drops sharply at $g \simeq 1$ and, at large $g \gg 1$, behaves as $T_{\text{BKT}} \sim E_c g \exp\{-g\}$. As shown in Appendix B, the disagreement is not a consequence of the different model we use, but can be traced back to the disregard of the quantum fluctuations of phase in the earlier works. By contrast, Ref. [4] uses a perturbative renormalization scheme that neglects instanton configurations. However, it is precisely these instanton configurations that reflect the discreteness of charge which is the key point in identifying the transition.

In the presence of the self-capacitance, $C > 0$, the screening length $\xi_s \simeq \sqrt{1 + C'/C} \exp\{g/2\}$ is finite, and the transition is smeared into a crossover. The crossover is sharp as long as $\xi_s \gg 1$. Regardless of the ratio C'/C' , this is the case for $g \gg 1$. In this regime the charge gap is parametrically larger than the crossover temperature, $\Delta \simeq gT_{\text{BKT}}$, and therefore the residual conductivity below the crossover, though finite, is exponentially small, $\sigma \lesssim g \exp\{-g\}$. As a result, quantitatively, there is little difference between the models with and without

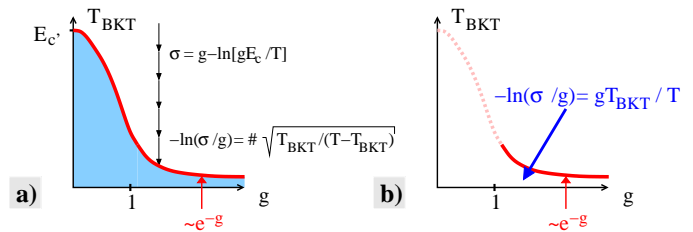


FIG. 2: BKT temperature as a function of g . For $g \gg 1$, T_{BKT} is exponentially small, but remains finite. a) $C = 0$: the true transition exists for any value of g . Conductance is zero below the transition temperature. b) $C > 0$: crossover takes place. It is sharp only if $g \gg 1$ and/or $C' \gg C$. In the regime $T < T_{\text{BKT}}$, the system shows activation behavior with the gap $\Delta = T_{\text{BKT}} \ln(\xi_s^2)$.

self-capacitance. This is not the case for $g \lesssim 1$: unless $C' \gg C$, the crossover is gone, and the conductivity follows the simple activation law $\sigma \simeq g \exp\{-\Delta/T\}$ with $\Delta \simeq E_c$.

IV. FINITE GATE VOLTAGE

So far we have restricted ourselves to the case of zero gate voltage only. A finite gate voltage induces a continuous background charge $q \propto V_{\text{gate}}$ on the grains. In this case the charging term in the action Eq. (8) has to be replaced with $S_{\text{cl}}^{(c)}[\vec{\theta}; q] = E_c/T \sum_{\mathbf{l}} (\nabla \cdot \vec{\theta}_{\mathbf{l}} - q)^2$. Alternatively one may shift the $\vec{\theta}$ field by $q\mathbf{l}$ to move the q -dependence into the pinning term $\frac{\gamma(T)}{2\pi^2} \cos(2\pi(\theta_i + ql_i))$. Since grain coordinates l_i take only integer values, the model is periodic in the q -space with unit period. In this work we restrict ourselves to a uniform gate voltage $q(\mathbf{l}) = q = \text{const}$, leaving considerations of a random background charge for future studies.

For small q , the system is in a particle-hole symmetric “neutral” state: the ground state is still (as for $q = 0$) characterized by $\vec{\theta}_1 = 0$. At some finite value $q = q^*$, a transition takes place, where the ground state becomes charged (with a non-integer average number of electrons per dot) and spatially non-uniform. To find q^* , let us compute the soliton energy in the presence of q . Since the q -dependence of the Hamiltonian is a pure boundary effect, one immediately finds the soliton energy $\Delta(q) = \Delta(0) - 2qE_c$. At $q^* = \Delta(0)/(2E_c)$ the soliton energy $\Delta(q)$ vanishes. This marks the transition into the charged state: for $q > q^*$, solitons are created at no cost.

In the charged phase, the density of solitons in the array is finite even at zero temperature. In order to find the soliton density at $q > q^*$, one has to take into account interaction between the solitons. At small densities, $n_s < \xi_s^{-2} = \gamma$, the interaction between solitons is exponentially weak. The energy cost associated with a soliton density

n_s reads

$$E_{<}(n_s) = n_s \Delta(q) + \frac{2}{\pi} E_c \gamma n_s K_0 \left(\sqrt{\frac{\gamma}{n_s}} \right), \quad (16)$$

where the second contribution is given by the interaction energy of a pair of solitons separated by the distance $1/\sqrt{n_s}$, multiplied by the soliton density. Since $\sqrt{\gamma/n_s} \gg 1$, we can use the asymptotic expression for the Bessel function, $K_0(x) \sim x^{-1/2} \exp\{-x\}$ for $x \rightarrow \infty$. The optimal density is determined by the minimum of $E_{<}(n_s)$. Minimization of $E_{<}(n_s)$ with respect to n_s yields $n_s(q) \sim \gamma / \ln^2[\gamma/(q - q^*)]$, where we used that $\Delta(q) = 2E_c(q^* - q)$. Thus, at $q \gtrsim q^*$, the soliton density rises rapidly until at $q - q^* \simeq \gamma$, the distance between solitons reaches ξ_s . For $n_s > \xi_s^{-2}$, the solitons start to interact logarithmically. Consequently, the expression for the energy has to be modified as

$$\begin{aligned} E_{>}(n_s) &= n_s \Delta(q) + \frac{1}{2\pi} E_c \gamma n_s^2 \int_{1/\sqrt{n_s}}^{\infty} l dl K_0(\sqrt{\gamma} l) \\ &\simeq n_s \Delta(q) + \frac{1}{2\pi} E_c n_s \left(n_s - \gamma \ln \sqrt{\frac{n_s}{\gamma}} \right), \end{aligned} \quad (17)$$

where the second contribution describes the interaction energy of the solitons with density n_s ; in the volume $\xi_s^2 = 1/\gamma$, the interaction is logarithmic [$K_0(x) \simeq -\ln x$ for $x \ll 1$]. In this regime, the minimization yields $n_s(q) \sim 2\pi(q - q^*) + (\gamma/4) \ln[(q - q^*)/\gamma]$ for $q - q^* \gg \gamma$.

Naively, one would expect the system to be no longer insulating once the density of solitons becomes finite at $q > q^*$ – which would be the case if the solitons were mobile. However, even though the soliton density in the system is finite, $n_s > 0$, it turns out that – except for a narrow region $q - q^* < \gamma$, where the interaction between solitons is exponentially weak – the solitons form a Wigner crystal which is pinned due to the underlying lattice structure. Thus, transport is still activated.

To understand this fact, we use the analogy with the formation of vortices in a type II superconducting film²⁰. The field $\vec{\theta}$ may be viewed as $\mathbf{A} \times \mathbf{n}_z$, where \mathbf{A} is the vector potential and \mathbf{n}_z is a unit vector normal to the film. Since the local magnetic field is given as $\mathbf{h} = h \mathbf{n}_z = \nabla \times \mathbf{A}$, the correspondence goes as $\nabla \cdot \theta = h$ and the charge quantization in the array is equivalent of the flux quantization in the superconductor, $\int (d^2l) h = k$ ($k \in \mathbb{Z}$), where h is measured in units of the flux quantum ϕ_0 . In this analogy, the gate voltage translates to the external magnetic field, H , and the gate voltage q^* corresponds to the critical magnetic field H_{c1} , where it becomes energetically favorable to create vortices. The correspondences are summarized in the following “dictionary”:

array	superconducting film
$\vec{\theta}$	$\mathbf{A} \times \mathbf{n}_z = -\lambda^2 \nabla h$
charge $\nabla \cdot \vec{\theta}$	local magnetic field h
$\xi_s = 1/\sqrt{\gamma}$	penetration depth λ
background charge q	external magnetic field H
q^*	H_{c1}

Above H_{c1} there is a finite density of vortices in the system which at low enough temperatures form an Abrikosov lattice²¹. In a clean film, the vortex lattice is free to move, but it is easily pinned by the system boundaries, the underlying lattice structure (as in Josephson junction arrays) or any sort of disorder. Upon increasing the temperature the vortex lattice eventually melts^{11,14}, and above the melting temperature T_m most of the vortices are free to move. The melting temperature at finite $H > H_{c1}$ is smaller than, but parametrically the same as the Berezinskii–Kosterlitz–Thouless temperature at zero magnetic field¹⁴. Thus, at $T < T_m$ the system is superconducting while at $T > T_m$ the moving vortices lead to dissipation.

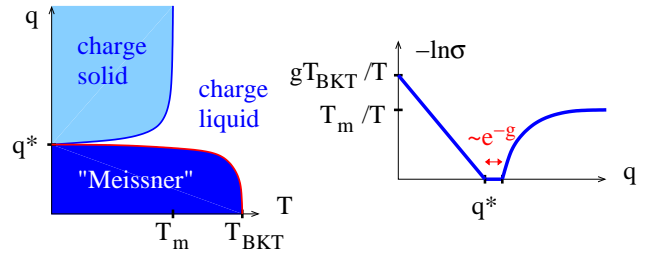


FIG. 3: System properties as a function of an external gate voltage. The system becomes charged at $q > q^*$. If the soliton density is larger than $1/\xi_s^2$, charges arrange into a (pinned) Wigner crystal. a) Phase diagram. b) Conductivity at $T < T_m$ as a function of q .

Translating back to our problem this means that at $q > q^*$ the solitons form a Wigner crystal once their density is sufficiently large such that the interaction is logarithmic. Only in the narrow interval $q^* < q < q^* + \xi_s^{-2}$ the system is in the conducting charge liquid state. Upon increasing the gate voltage, the Wigner crystal forms and, due to lattice pinning, the system is an insulator at temperatures smaller than the melting temperature. The latter is of the order of T_{BKT} . Note that while for $q < q^*$ charge is carried by individual (thermally-activated) solitons, for $q > q^*$ the mobile charges are lattice defects, whose core energy is proportional to the logarithm of the lattice constant of the Wigner crystal.

V. CONCLUSIONS

The conductivity of a granular material with small ($g \ll 1$) inter-grain conductances is controlled by the Coulomb blockade effect in separate grains⁸. Charge transport in such an array occurs by electron hops between single grains. Because of the Coulomb blockade,

the granular array behaves as an insulator at low temperatures. The characteristic energy determining the activation of the charge transport, is associated with the single-grain charging energy E_c .

In this paper, we investigated the properties of a granular array at high inter-grain conductance, $g \gg 1$. We concentrated on the simplest model, neglecting the spacing between the discrete electron levels in the grains ($\delta \rightarrow 0$), and in the main part of the paper we also assumed the ideal limit of zero background charge ($q = 0$). We found that the granular array at sufficiently low temperatures remains an insulator even in the case of $g \gg 1$. The large inter-grain conductance, however, does affect the nature of the charge carrier. Instead of an integer (in the units of e) uncompensated charge sitting on a single grain, it is rather a charge- e soliton involving many grains. There is a sharp crossover to low conductance at temperature the $T_{\text{BKT}} \propto E_c \exp\{-g\}$. Below the crossover, the electron transport is associated with the activation of solitons with charges $\pm e$; the corresponding activation energy is relatively high, $\Delta \simeq gT_{\text{BKT}}$. The approach to the crossover region from the high-temperature side can be described in terms of the correlation radius for the Berezinskii-Kosterlitz-Thouless transition, see Eq. (2). Comparison of Eqs. (1) and (2) shows that the crossover width is $\delta T \sim T_{\text{BKT}}/g^2 \ll T_{\text{BKT}}$.

The effect of a gate voltage q applied uniformly throughout the array is to much extent similar to that of an external magnetic field applied to a type II superconductor. Until q reaches a certain critical value q^* the system's behavior does not change qualitatively (that is, it exhibits the BKT crossover from insulator to metal). The charge gap, Δ , and the crossover temperature, T_{BKT} , decrease with increasing q . At $q = q^*$ the gap vanishes (while the crossover temperature remains finite), and for even larger gate voltages there is a certain ground-state density, $n_s = n_s(q)$, of charge solitons. As long as this density is small $n_s(q) < \xi_s^{-2}$ the solitons are in a liquid state and the array conducts. At larger density, $n_s(q) > \xi_s^{-2}$, the solitons form a Wigner crystal pinned by the lattice. As a result, the array is again in the insulating state with the charge gap determined by the cost of a defect in the Wigner crystal.

Finally, let us mention related issues that are *not* addressed in the present paper. The first one is the role of disorder. The most relevant is charge disorder equivalent to a grain-dependent gate voltage q_1 . In the extreme scenario one may assume that q_1 are independent random variables, uniformly distributed in $[0, 1]$. One would then like to solve the classical statistical problem formulated by Eqs. (13) and (14) with random q_1 in the argument of $\sin(2\pi(\theta_{i,1} + q_1))$. Despite many similarities with the vortex physics, one can not simply transfer the known results from the pinned vortex lattice literature²². The reason is that random charge, q_1 , translates into a strong (of order of H_{c2}) fluctuating magnetic field, rather a than fluctuating pinning potential.

Another unaddressed issue is the role of quantum co-

herence, which enters the problem through the mean level spacing δ . Our results are valid as long as $g^2\delta \lesssim T_{\text{BKT}}$. In the opposite limit, the quantum coherence effects (most notably Anderson localization) start to interfere with the effects of electron-electron interactions, considered here. One may expect that both effects drive the system towards the insulating ground-state. (It is worth mentioning that in both cases the characteristic length happens to be exponentially large in the bare conductance, g .) The structure of such insulator is not known currently.

Acknowledgments

We are grateful to A. Altland for valuable discussions. This work was supported by NSF grants DMR01-20702, DMR02-37296, and EIA02-10736. Furthermore, JSM was supported by a Feodor Lynen fellowship of the Humboldt Foundation. AK and JSM acknowledge the hospitality of KITP (UCSB), where part of this research was done under NSF grant PHY99-07949.

APPENDIX A: MULTI-CHANNEL CONTACTS

In the main text (Sec. IIB), we derived a classical model for the single-channel case. Here we discuss its generalization to $N \geq 2$ channels. For every channel $\alpha = 1, \dots, N$ of a multi-channel contact, one introduces a field $\theta_\alpha(\tau)$. Consider an $M \times M$ array with N channels in each of the $2M^2$ contacts. The quadratic part of the action reads

$$S_2 = \frac{1}{T} \sum_{1,m} \left(\pi |\omega_m| \sum_{\alpha} \bar{\theta}_{1,\alpha}^2 + E_c \left(\sum_{\alpha} \nabla \cdot \bar{\theta}_{1,\alpha} \right)^2 \right), \quad (\text{A1})$$

while the backscattering is described by

$$S_r = -\frac{E_c}{\pi} \sum_{1,\alpha} \sum_{i=x,y} r_{i1\alpha} \int_0^\beta d\tau \cos(2\pi\theta_{i,1,\alpha}), \quad (\text{A2})$$

where the high-energy modes $E_c < |\omega_m| < D$ have already been integrated out. [At energies larger than E_c , all modes are decoupled and, thus, can be integrated out for each channel separately.] Here, in order to clarify the following evaluation scheme, the reflection coefficients r have been given indices specifying the direction, contact, and channel.

Only the $2M^2$ symmetric modes $\theta_1 = \sum_{\alpha} \theta_{1,\alpha}$ couple to external parameters, such as gate voltages. We want, thus, to find an effective action for θ_1 by integrating out $2M^2(N-1)$ asymmetric modes. To this end let us change variables from $\theta_{1,\alpha}$ ($\alpha = 1 \dots N$) to θ_1 and $\tilde{\theta}_{1,\alpha} = \theta_{1,\alpha} - (\theta_1 - \sum_{\alpha' > \alpha} \theta_{1,\alpha'}) / (\alpha + 1)$ ($\alpha, \alpha' = 1 \dots N-1$). While the symmetric fields θ_1 are massive due to the charging term, all the asymmetric fields $\tilde{\theta}_{1,\alpha}$ are massless.

As a result, the perturbation theory in powers of $r_{i\alpha}$ contains only the terms that do not have massless fields $\tilde{\theta}_{1,\alpha}$ in the exponents (cosines). Rewriting the backscattering action in terms of the new fields, one can see that

$$Z_N \sim E_c^N \prod_{\alpha=1}^N r_{i\alpha} \int d\tau_\alpha \cos \left(\frac{2\pi}{N} \sum_{\alpha} \theta_{i,1}(\tau_\alpha) \right) \prod_{\alpha=1}^N \left\langle \exp \left\{ 2\pi i \left(\tilde{\theta}_{i,1\alpha}(\tau_\alpha) - \frac{1}{\alpha} \left(\tilde{\theta}_{i,1,\alpha}(\tau_N) + \sum_{\alpha' < \alpha} \tilde{\theta}_{i,1,\alpha}(\tau_{\alpha'}) \right) \right) \right\} \right\rangle_{\tilde{\theta}_{1,\alpha}}.$$

Taking the averages $\langle \dots \rangle_{\tilde{\theta}_{1,\alpha}}$ with the actions

$$S[\theta_{i,1,\alpha}] = \frac{1}{T} \sum_m \frac{\alpha+1}{\alpha} \pi |\omega_m| \tilde{\theta}_{i,1,\alpha}^2, \quad (\text{A3})$$

$$S[\vec{\theta}] = \sum_1 \left\{ \frac{1}{T} \sum_m \left(\frac{\pi}{N} |\omega_m| \vec{\theta}_1^2 + E_c (\nabla \cdot \vec{\theta}_1)^2 \right) - \frac{E_c}{\pi} \sum_{i=x,y} \prod_{\alpha=1}^N r_{i\alpha} \int d\tau_\alpha \prod_{\alpha' > \alpha} \frac{1}{(\tau_\alpha - \tau_{\alpha'})^{2/N}} \cos \left(\frac{2\pi}{N} \sum_{\alpha} \theta_{i,1}(\tau_\alpha) \right) \right\}. \quad (\text{A4})$$

Note that it is important to keep the non-local in time structure of the cosine-term.

At this stage, we can proceed to integrate out all the remaining modes except the static one, $\theta_{m=0}$ – as in the single-channel case. The prefactor of the cosine-term $V_0 = (E_c/\pi) \prod_{\alpha} r_{i\alpha}$ is renormalized according to

$$\begin{aligned} V_0 &\rightarrow V(T) = V_0 \exp \left\{ - \frac{2\pi^2}{N^2} \sum_{\alpha, \alpha'} \langle \theta(\tau_\alpha) \theta(\tau_{\alpha'}) \rangle_{\theta_{m \neq 0}} \right\} \\ &= V_0 \exp \left\{ - \sum_{m \neq 0} f(\omega_m) \left(1 + \frac{2}{N} \sum_{\alpha, \alpha' > \alpha} \cos \omega_m \tau_{\alpha\alpha'} \right) \right\}, \end{aligned}$$

where $f(\omega_m) = T/(4M^2) \sum_{\mathbf{q}} \{ (E_{\mathbf{q}} + \pi |\omega_m|)^{-1} + (\pi |\omega_m|)^{-1} \}$; see section II. Since typical time differences $\tau_{\alpha\alpha'} = \tau_\alpha - \tau_{\alpha'}$ are of the order $1/T$ (the time integrals are dominated by the upper limit of integration), the last cosine-term inside the exponent may be disregarded. As a result we find $V(T) = V_0 \sqrt{T/E_c}$.

Finally, one may perform the multiple time integrations in the prefactor of the cosine. The integral over the center-of-mass time $\tau = \sum_{\alpha} \tau_\alpha / N$ contributes a factor $1/T$, while the integration over $N-1$ independent time differences $\tau_\alpha - \tau$ yields a constant c_N multiplied by the logarithmic factor¹⁸ $\ln E_c/T$. The latter follows simply from power counting. The same logarithmic factor appears in the framework of the phase model, Appendix B, as a result of zero-mode integration. Since all our evaluations of γ are done up to a numerical factor, we shall not keep this logarithm explicitly. We, thus, reproduce Eq. (8) with $\gamma(T) \sim \sqrt{T/E_c} \prod_{\alpha=1}^N r_\alpha$. Continuation to

the lowest order non-vanishing terms are of the order $\prod_{\alpha=1}^N r_{i\alpha}$, where the product runs over *all* channels of a given contact:

yields $E_c^{1-N} \prod_{\alpha=1}^N \prod_{\alpha' > \alpha} (\tau_\alpha - \tau_{\alpha'})^{-2/N}$ for the product of correlators $\prod_{\alpha} \langle \dots \rangle_{\tilde{\theta}_{1,\alpha}}$.

Thus, the effective action for $\vec{\theta}_1$ reads

$T < T_0$ follows the same way as discussed in the main text for the single-channel case.

APPENDIX B: PHASE MODEL

In this Appendix, we establish correspondence between the charge representation, employed in the paper, and the more commonly used phase model. The latter may be straightforwardly derived starting from the fermionic tunneling Hamiltonian. Integration over the fermionic degrees of freedom (under the assumption of vanishing level spacing in every grain, $\delta \rightarrow 0$), leads to a model formulated in terms of the dynamic phase variable²³, $\phi_1(\tau)$. Its time derivative, $\dot{\phi}_1(\tau)$, has the meaning of a fluctuating instantaneous voltage on grain 1. The resulting action is a straightforward generalization of the Ambegaokar-Eckern-Schön (AES) action²³ to the array geometry. It consists of the charging term,

$$S_c[\phi] = \int_0^\beta d\tau \sum_1 \left[\frac{\dot{\phi}_1^2}{4E_c} - iq\dot{\phi}_1 \right], \quad (\text{B1})$$

and the dissipative term

$$S_d[\phi] = \frac{gT^2}{4} \int_0^\beta \int_0^\beta d\tau d\tau' \sum_{\langle 1, 1' \rangle} \frac{\sin^2(\phi_{1\mathbf{V}}(\tau) - \phi_{1\mathbf{V}}(\tau'))}{\sin^2(\pi T(\tau - \tau'))}, \quad (\text{B2})$$

describing tunneling between nearest neighbor grains $\langle 1, 1' \rangle$. Here, $\phi_{1\mathbf{V}} = (\phi_1 - \phi_{1'})/2$.

The phase field $\phi_1(\tau)$ obeys the boundary condition $\phi_1(\beta) - \phi_1(0) = 2\pi W_1$, where $W_1 \in \mathbb{Z}$ is an integer called winding number. In addition to the trivial configuration $\phi_1 = 0$, the stationary configurations of the dissipative action, S_d , are given by Korshunov instantons²⁴

$$e^{i\phi_1^{(W_1)}} = \prod_{a=1}^{|W_1|} \frac{e^{2\pi i \tau T - z_a}}{1 - \bar{z}_a e^{2\pi i \tau T}} \quad (\text{B3})$$

characterized by the spatially-dependent winding number W_1 and a set of complex parameters $|z_a| < 1$. In the regime $T \ll E_c$, these configurations are a good approximation to the saddle points of the total action. In the same approximation the z_a are zero-mode coordinates: the instanton action is almost z -independent (safe for the charging terms that weakly depends on z). Neglecting this dependence, the action for a certain winding number configuration, $\{W_1\}$, reads

$$S_W \simeq \frac{\pi^2 T}{E_c} \sum_{\mathbf{l}} W_{\mathbf{l}}^2 + \frac{g}{4} \sum_{\langle \mathbf{l}, \mathbf{l}' \rangle} |W_{\mathbf{l}} - W_{\mathbf{l}'}|, \quad (\text{B4})$$

where $W_{\mathbf{l}'} \equiv W_1 - W_{\mathbf{l}}$. In the regime, we are interested in, $T \ll E_c$ and $g \gg 1$, the dominant contribution comes from the second (tunneling) term in this expression. Since the latter depends only on the differences of winding numbers on neighboring grains, it favors configurations with spatially extended regions with a fixed constant winding number, e.g. $W_1 = \pm 1$ for a closed set of grains \mathbf{l} . We shall refer to such sets of grains with a fixed non-zero winding number as ‘‘islands’’. A typical phase-field configuration contains, therefore, a number of ‘‘islands’’ (with fixed non-zero windings) embedded in the sea of $W = 0$ grains. An example of such a configuration is shown in Fig. 4. According to Eq. (B4), the action cost of one such island with the winding number W is $S = AW^2(\pi^2 T/E_c) + L|W|(g/2)$, where A is the area of the island (number of grains inside) and L is its circumference (number of contacts with a winding number jump across them).

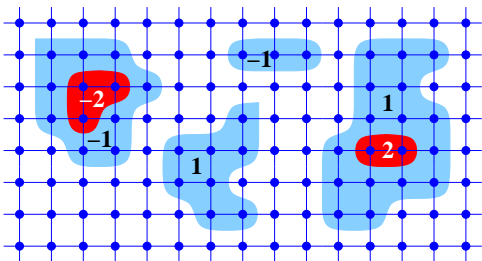


FIG. 4: A typical island configuration is shown. The numbers correspond to winding numbers in the phase model.

The same picture was employed in previous studies of 2d granular arrays^{7,8}, where the island structure was mapped onto the, so called, solid-on-solid model. The latter is known to exhibit a BKT transition. [A true transition takes place if there is no cost for the island’s area,

as is the case for the model with mutual capacitances only. Indeed, in such a model both charging and tunneling terms provide a cost proportional to the island’s circumference, L . In presence of the self-capacitance (and thus an area-proportional cost) the transition is smeared into a crossover.] What was missed in the previous studies is an account of fluctuations on top of the stationary island-like configurations.

We provide such an account here. Consider a stationary configuration consisting of a single island with a fixed winding number W . Expanding to the second order in deviations $\phi_1 = \phi_1^{(W_1)} + \varphi_1$, one finds for the fluctuating part of the action

$$\delta S = \sum_m \sum_{\mathbf{l}, \mathbf{l}'} \bar{\varphi}_{\mathbf{l}, m} M_{\mathbf{l}, \mathbf{l}', m}^{(W)} \varphi_{\mathbf{l}', m}, \quad (\text{B5})$$

where m is a Matsubara index, and $M_{\mathbf{l}, \mathbf{l}', m}^{(W)} \equiv \mathbf{M}_m^{(W)}$ is the fluctuation matrix. The fluctuation factor associated with this configuration is given by

$$\prod_{m>1} \frac{\det \mathbf{M}_m^{(0)}}{\det \mathbf{M}_m^{(W)}} = \exp \left\{ - \sum_m \text{Tr} \ln \left(\mathbf{M}_m^{(0)} \right)^{-1} \mathbf{M}_m^{(W)} \right\}, \quad (\text{B6})$$

where $\mathbf{M}_m^{(0)}$ is the corresponding fluctuation matrix for the flat ($W = 0$) stationary configuration. In the regime $g \gg 1$, the dominant fluctuation contribution comes from the expansion of the tunneling term, S_d . This leads to $M_{\mathbf{l}, \mathbf{l}', m}^{(0)} = -g|\omega_m|$ for nearest neighbors $\langle \mathbf{l}, \mathbf{l}' \rangle$, while $M_{\mathbf{l}, \mathbf{l}, m}^{(0)} = -\sum_{\mathbf{l}' \neq \mathbf{l}} M_{\mathbf{l}, \mathbf{l}', m}^{(0)}$ and $M_{\mathbf{l}, \mathbf{l}', m}^{(0)} = 0$ otherwise. In presence of the island, the off-diagonal elements of the fluctuation matrix are changed to $M_{\mathbf{l}, \mathbf{l}', m}^{(W)} = -g|\omega_{m-|W|}$ (and the diagonal elements accordingly), only if \mathbf{l} and \mathbf{l}' are nearest neighbors laying across the island’s boundary. As a result, one may write $\mathbf{M}_m^{(W)} = \mathbf{M}_m^{(0)} - |W|\delta\mathbf{M}$, where the matrix $\delta\mathbf{M}$ has entries $\pm 2\pi Tg$ along the island’s boundary and zeros everywhere else. Returning to the calculation of the fluctuation factor, Eq. (B6), one finds $\text{Tr} \ln \left(\mathbf{M}_m^{(0)} \right)^{-1} \mathbf{M}_m^{(W)} = \text{Tr} \ln \left[1 - |W| \left(\mathbf{M}_m^{(0)} \right)^{-1} \delta\mathbf{M} \right] \approx -|W| \text{Tr} \left(\mathbf{M}_m^{(0)} \right)^{-1} \delta\mathbf{M}$. Higher order terms in the expansion of the logarithm are rapidly convergent upon Matsubara summation and, therefore, may be safely neglected. Since $\mathbf{M}_m^{(0)} \sim g|\omega_m|$, summation over the Matsubara index in $\sum_m |W| \text{Tr} \left(\mathbf{M}_m^{(0)} \right)^{-1} \delta\mathbf{M}$ leads to the logarithmic divergence²⁵. It is cut off by the charging part of the action at $m \approx gE_c/T \gg 1$. The summation (trace) over spatial indices results in a factor proportional to L , the island’s circumference, as it counts the number of non-zero entries in $\delta\mathbf{M}$. Finally, a careful evaluation of the numerical coefficient²⁶ leads to the fluctuation factor, Eq. (B6), equal to $(gE_c/T)^{L|W|/2}$.

As a result, an island of winding number W with area A and circumference L contributes to the partition func-

tion of the model with the relative factor

$$P_W(A, L) = \left(e^{-\pi^2 T/E_c} \right)^{AW^2} \left(\sqrt{\frac{gE_c}{T}} e^{-g/2} \right)^{L|W|}. \quad (\text{B7})$$

(Actually, the statistical weight of an island contains also a factor $(\ln E_c/T)^{|W|}$, coming from the zero-mode, z_a , integrations²⁵. This factor has its exact analog in the charge model, mentioned at the end of Appendix A. Hereafter we omit it for brevity.)

We shall show now that the perturbative expansion in powers of $\gamma(T)$ of the classical model, Eq. (8), leads to the same island picture. In this case, every island carries the relative factor $\tilde{P}_W(A, L) = \left(e^{-\pi^2 T/E_c} \right)^{AW^2} (E_c \gamma(T)/(2\pi^2 T))^{L|W|}$. We can, thus, identify the two models provided $\gamma(T) \simeq \sqrt{gT/E_c} e^{-g/2}$. Notice that $\gamma(T) \propto \sqrt{T/E_c}$ is exactly what one expects for the high-temperature, $T > T_0$, charge model. At lower temperature, non-linear fluctuation corrections in the phase model diverge⁴ and the above treatment runs out of validity. However, having established the equivalence of the phase and charge models at $T > T_0$, one may proceed with the analysis of the latter even at smaller temperatures.

To complete the proof, we elucidate now the island structure of the perturbative expansion of the charge model, Eq. (8). Consider the expansion of the partition function $\mathcal{Z} = \int D\vec{\theta} \exp\{-S[\vec{\theta}]\}$, with the action $S[\vec{\theta}]$ given by Eq. (8), in powers of the small parameter γ . The partition function can be written as $\mathcal{Z} = \sum_{n=0}^{\infty} Z_n (E_c \gamma/T)^n$, where Z_n is a product of n cosine terms averaged with the action $S_c[\vec{\theta}] = E_c \sum_{\mathbf{l}} (\nabla \cdot \vec{\theta}_{\mathbf{l}})^2/T$. There are two types of contributions: a) terms with higher powers of the cosine taken at the same link and b) terms involving different links. The first class of terms describes perturbative corrections to the conductance of a single contact, and may be shown to be equivalent to those of Ref. [4] in the framework of the phase model.

The second class corresponds to the instanton terms and is the subject of our focus. These terms exhibit ‘‘island formation’’. To illustrate this, let us label the coefficients $\gamma_{i,\mathbf{l}}$ (even though we assume them all to be equal), where $i = x, y$. Terms of the form $\prod_{\underline{\alpha}} \gamma_{\underline{\alpha}}$ are non-zero only if the lines crossing all contacts $\underline{\alpha} = (i, \mathbf{l})$ form closed loops, see Fig. 4. I.e. the lowest-order non-local term is proportional to $\gamma^4 = \gamma_{x,\mathbf{l}} \gamma_{x,\mathbf{l}+\mathbf{e}_x} \gamma_{y,\mathbf{l}} \gamma_{y,\mathbf{l}+\mathbf{e}_y}$ – involving all the four links surrounding grain **1**. This property of the model is due to the presence of massless modes, as is explained below.

Rewriting $\vec{\theta} = \nabla \chi + \nabla \times \eta$, one finds that the charging action takes the form $S_c[\chi, \eta] = E_c \sum_{\mathbf{l}} (\nabla \chi_{\mathbf{l}})^2/T$ and is thus η -independent. The rotational field η is therefore strictly massless. As a result, as long as an argument of the cosine (exponential) function contains the η -field, it averages to zero. Indeed, to obtain Z_n one has to average expressions of the form $\exp\{2\pi i (\sum_{j_x=1}^s (\pm) \theta_{x,\mathbf{l}_{j_x}} + \sum_{j_y=s+1}^n (\pm) \theta_{y,\mathbf{l}_{j_y}})\}$, where j_i labels contacts in i -direction. The terms containing η in the argument of this exponent, vanish. Therefore non-vanishing are only those terms that have $\sum_{j_x} \pm (\eta_{\mathbf{l}_{j_x}} - \eta_{\mathbf{l}_{j_x}-\mathbf{e}_x}) + \sum_{j_y} \pm (\eta_{\mathbf{l}_{j_y}} - \eta_{\mathbf{l}_{j_y}-\mathbf{e}_x}) = 0$. It can be seen that this condition corresponds to the island structure. As a result, every island brings a factor $(E_c \gamma/T)^L$, where L is its circumference, that simply reflects the order of the perturbation theory needed to create the island. For a proper (i.e. island-like) term of the perturbation theory, the averaging over the massive χ -fields results in the factor $\exp\{-\pi^2 T A/E_c\}$, where A is the area. Finally, the integer index $|W|$ corresponds to the possibility of having a non-zero term of the perturbation theory, where links surrounding an island are included $|W|$ times each. We have shown, thus, that the perturbation theory in the charge model, Eq. (8), produces the same island structure as the instanton expansion of the phase model – with the same relative factors, Eq. (B7). This completes the proof of the equivalence of the two models and provides the value of $\gamma(T)$, Eq. (9), for $g \gg 1$.

¹ A. Gerber, A. Milner, G. Deutscher, M. Karpovsky, and A. Gladkikh, Phys. Rev. Lett. **78**, 4277 (1997).

² D.S. Golubev and A.D. Zaikin, Phys. Lett. **A169**, 475 (1992); G. Goepfert and H. Grabert, Euro. Phys. J. B **16**, 687 (2000).

³ I.S. Beloborodov, K.B. Efetov, A. Altland, and F.W.J. Hekking, Phys. Rev. B **63**, 115109 (2001).

⁴ K.B. Efetov and A. Tschersich, Europhys. Lett. **59**, 114 (2002).

⁵ A. Altland, L.I. Glazman, and A. Kamenev, Phys. Rev. Lett. **92**, 026801 (2004).

⁶ B.L. Altshuler, A.G. Aronov, and D.E. Khmel'nitskii, J. Phys. C **15**, 7367 (1982).

⁷ J.E. Mooij, B.J. van Wees, L.J. Geerligs, M. Peters, R. Fazio, and G. Schön, Phys. Rev. Lett. **65**, 645 (1990).

⁸ R. Fazio and G. Schön, Phys. Rev. B **43**, 5307 (1991).

⁹ I.S. Beloborodov, K.B. Efetov, A.V. Lopatin, and V.M. Vinokur, Phys. Rev. Lett. **91**, 246801 (2003).

¹⁰ B.L. Altshuler and A.G. Aronov, in *Electron-Electron Interaction In Disordered Systems*, eds. A.J. Efros and M. Pollak, pp. 1-153, Elsevier, North-Holland, 1985.

¹¹ J.M. Kosterlitz and D.J. Thouless, J. Phys. C **6**, 1181 (1973).

¹² V.L. Berezinskii, Zh. Eksp. Teor. Fiz. **59**, 907 (1970) [Sov. Phys. JETP **32**, 493 (1971)].

¹³ J.E. Mooij, in *Percolation, Localization, and Superconductivity*, NATO ASI Series B, Vol. 109, eds. A.M. Goldman and S.A. Wolf, pp. 325-370, Plenum Press, 1983.

¹⁴ B.A. Huberman and S. Doniach, Phys. Rev. Lett. **43**, 950 (1979); D.S. Fisher, Phys. Rev. B **22**, 1190 (1980).

- ¹⁵ K. Flensberg, Phys. Rev. B **48**, 11156 (1993).
- ¹⁶ K.A. Matveev, Phys. Rev. B **51**, 1743 (1995); A. Furusaki and K.A. Matveev, Phys. Rev. B **52**, 16676 (1995).
- ¹⁷ Yu.V. Nazarov, Phys. Rev. Lett. **82**, 1245 (1999).
- ¹⁸ I.L. Aleiner, P.W. Brouwer, and L.I. Glazman, Phys. Rep. **358**, 309 (2002).
- ¹⁹ A. Kamenev, in Nato Science Series II, Vol. 72, eds. I.V. Lerner *et al.*, pp. 313-340, Kluwer Academic Publishers, Dordrecht, 2002.
- ²⁰ P.G. de Gennes, *Superconductivity of Metals and Alloys*, W.A. Benjamin, New York, 1966.
- ²¹ A.A. Abrikosov, Zh. Eksp. Teor. Fiz. **32**, 1442 (1957) [Sov. Phys. JETP **5**, 1174 (1957)].
- ²² G. Blatter, M.V. Feigel'man, V.B. Geshkenbein, A.I. Larkin, and V.M. Vinokur, Rev. Mod. Phys. **66**, 1125 (1994).
- ²³ V. Ambegaokar, U. Eckern, and G. Schön, Phys. Rev. Lett. **48**, 1745 (1982); G. Schön and A.D. Zaikin, Phys. Rep. **198**, 237 (1990).
- ²⁴ S.E. Korshunov, Pis'ma Zh. Eksp. Teor. Fiz. **45**, 342 (1987) [JETP Lett. **45**, 434 (1987)].
- ²⁵ X. Wang and H. Grabert, Phys. Rev. B **53**, 12621 (1996); M.V. Feigel'man, A. Kamenev, A.I. Larkin, and M.A. Skvortsov, Phys. Rev. B **66**, 054502 (2002).
- ²⁶ A. Altland, L.I. Glazman, A. Kamenev, and J.S. Meyer, unpublished.